Pakistan Veterinary Journal

ISSN: 0253-8318 (PRINT), 2074-7764 (ONLINE)
DOI: 10.29261/pakvetj/2024.252

RESEARCH ARTICLE

Mycogenic Zinc Nanoparticles with Antimicrobial, Antioxidant, Antiviral, Anticancer and anti-Alzheimer Activities Mitigate the Aluminium Toxicity in Mice: Effects on Liver, Kidney, and Brain Health and Growth Performance

Hawazen K. Al-Gheffari[1], Salma M. Aljahdali[2], Mody Albalawi[3], Amnah Obidan[3], Najat Binothman[4], Majidah Aljadani[4], Nouf Aldawood[5], Nada F. Alahmady[6,7], Saif Saad Alqahtani[8], Abdullah M. Alkahtani[9], Aminah Allohibi[10], Widad Abu al-Khair[11], Khaled M. Wahdan[12], Nahla Alsayd Bouqellah[13*]

[1]Department of Biological Sciences, Faculty of Science, King Abdulaziz University, Jeddah, Saudi Arabia; [2]Department of Biochemistry, Faculty of Science, King Abdulaziz University, Jeddah, Saudi Arabia; [3]Department of Biochemistry, Faculty of Science, University of Tabuk, Tabuk, Kingdom of Saudi Arabia; [4]Department of Chemistry, College of Sciences & Arts, King Abdulaziz University, Rabigh 21911, Saudi Arabia; [5]Department of Biology, College of Science, Princess Nourah bint Abdulrahman University, P.O.Box 84428, Riyadh 11671, Saudi Arabia; [6]Department of Biology, College of Science, Imam Abdulrahman bin Faisal University, P. O. Box 1982, Dammam, 31441, Saudi Arabia; [7]Basic and Applied Scientific Research Center (BASRC), Imam Abdulrahman Bin Faisal University, PO Box 1982, Dammam 31441, Saudi Arabia; [8]Immunology and Flowcytometry Department, Riyadh Regional Laboratory, Riyadh 11425, Saudi Arabia; [9]Department of Microbiology & Clinical Parasitology, College of Medicine, King Khalid University, Abha, Saudi Arabia; [10]Biological Sciences Department, College of Science & Arts, King Abdulaziz University, Rabigh 21911, Saudi Arabia; [11]National Medical Research Center, Faculty of Science, Zawiya University, Libya; [12] Department of Agricultural Biochemistry, Faculty of Agriculture, Zagazig University, Zagazig 44511, Egypt; [13]Department of Biology, College of Science, Taibah University, Almadina Almunawwarah 42317-8599, Saudi Arabia
*Corresponding author: Nahla Alsayd Bouqellah (Nbouqellah@taibahu.edu.sa)

ARTICLE HISTORY (24-459)

Received:	August 3, 2024
Revised:	September 12, 2024
Accepted:	September 13, 2024
Published online:	September 27, 2024

Keywords:
Heavy metals
Contamination
Neurological diseases
Virus
Antioxidant
Cancer
oxidative stress
Diet
Mice

ABSTRACT

This study investigates the *in vitro* and *in vivo* biological activities of mycogenic Zn nanoparticles synthesized by *Aspergillus fumigatus* (AFZN) as an effective neurological, antioxidant, antibacterial, antiviral, and anticancer agents besides mitigating the Al toxicity in albino mice. The spherical AFZN were 39nm in size and -23.6mV charge; these properties possessed the antioxidant, anticancer, antibacterial, antiviral, and anti-alzheimer activities. The *in vitro* findings revealed that AFZN (100 µg/mL) significantly inhibited 89% of DPPH radicals, 84% of the activity of AChE, and 85% of brain cancer cell lines besides pathogenic bacteria. The obtained ZnNPs reduced the severity of the lumpy skin disease virus (LSDV) by 84%. The antioxidant and neurological activity of ZnNPs in $AlCl_3$-challenged mice were evaluated; therefore, 120 mice were allocated into six groups: control, three groups received ZnNPs concentrations (25, 50, and 75 mg/kg), $AlCl_3$-challenged group, and $AlCl_3$-challenged group and treated with ZnNPs (75 mg/kg). The dietary ZnNPs (75 mg/kg) significantly enhanced body weight gain, feed intake, and feed conversion ratio compared to the control and $AlCl_3$-challenged group. The liver enzymes (AST and ALT), uric acid, total cholesterol, LDL, and MDA were at a high level in $AlCl_3$-challenged groups, whereas ZnNPs (75 mg/kg) treatment enhanced the oxidative stability and immunity markers in the $AlCl_3$-challenged group, where decreased MDA, and enhanced the activity of the enzymatic defence system (SOD, CAT, and GPx). Also, it downregulated the brain, liver, and renal proinflammatory (OCCU and MUC-1, IL-6, and IL-1β) and pro-cancerous (Bax and caspase-3) markers in the $AlCl_3$-challenged group. The brain, liver, and kidney histology correlated with the results of biochemical parameters, where ZnNPs application recovered the tissue structure as control. It concluded that mycogenic ZnNPs can be used as an antioxidant and anti-alzheimer agent in the $AlCl_3$-challenged group.

To Cite This Article: Al-Gheffari HK, Aljahdali SM, Albalawi M, Obidan A, Binothman N, Aljadani M, Aldawood N, Alahmady NF, Alqahtani SS, Alkahtani AM, Allohibi A, Abu al-Khair W, Wahdan KM, Bouqellah NA, 2024. Mycogenic zinc nanoparticles with antimicrobial, antioxidant, antiviral, anticancer, and anti-alzheimer activities mitigate the aluminium toxicity in mice: effects on liver, kidney, and brain health and growth performance. Pak Vet J, 44(3): 763-775. http://dx.doi.org/10.29261/pakvetj/2024.252

INTRODUCTION

Nanotechnology has been incorporated into the veterinary domain as a tool for disease detection and the formation of innovative therapeutic and prophylactic strategies (Prasad *et al.,* 2021). Due to their small size and unique physicochemical properties, nanoparticles have become invaluable tools in biological applications. They offer precise drug delivery, controlled release, and the ability to manipulate the immune system within living organisms. Additionally, metal nanoparticles have shown promising antiviral, antibacterial, and antioxidant capabilities (Ermakov and Jovanović, 2022; Fatima *et al.,* 2024).

Zinc is essential for all living organisms (Mohd Yusof *et al.,* 2021). Additionally, Zn possesses antioxidant properties and plays a crucial role in the antioxidant defense system (Matuszczak *et al.,* 2024). Additionally, Zn is a constituent of several proteins that play a role in immune defense systems, hormone secretion pathways, and secondary metabolites (Ogbuewu and Mbajiorgu, 2023). Zinc nanoparticles (ZnNPs) are mineral salts with particle sizes ranging from 1 to 100 nm (Shaba *et al.,* 2021). Zinc nanoparticles can be produced through three primary methods: chemical, physical processes, and green synthesis. Among these, microbial-mediated synthesis is often considered a more environmentally friendly and safer alternative to traditional chemical and physical approaches (Gauba *et al.,* 2023). ZnNPs have attracted significant attention because of their small size, specific shape, expanded and enhanced surface area and activity, efficient catalytic properties, and powerful adsorption capabilities (Blinova *et al.,* 2020). These unique properties of ZnNPs have recently gathered significant interest.

Zinc nanoparticles have broad-spectrum antimicrobial properties against many pathogens. Zinc oxide nanoparticles have been used as nanoparticles for controlling and inhibiting many viruses at the vitro level, including bovine herpesvirus-1 (Zeedan *et al.,* 2020), H1N1 influenza virus (Ghaffari *et al.,* 2019), hepatitis C virus, hepatitis B virus (Kumar *et al.,* 2023), and Herpes Simplex Virus Type 1 (HSV-1) (Melk *et al.,* 2021).

Aluminum (Al) represents 8% of the earth's crust (Laabbar *et al.,* 2014). Al flexibility makes it useful in cookware, food packaging, water purification, and several medications, such as antidiarrheal agents, antacids, phosphate binders, antiperspirants, buffered aspirin, and cosmetics. These sources significantly contribute aluminum to the human body (Willhite *et al.,* 2014). It is believed that the amount of aluminum eaten daily from drinking water is around 160µg. However, this amount can be as high as 3.5-5.2g per day (equivalent to 50-75 mg/kg/day) due to the intake of aluminum-based antacids (Krupińska, 2020). High exposure to Al can impact the brain, bones, and functions of the spleen, liver, kidneys, and immune system (Gökmen and Gül, 2023).

Recent studies have indicated that aluminum can potentially be hazardous to the body's systems (Renke *et al.,* 2023). While aluminum is common in our environment, high levels of exposure have been linked to several health concerns, including neurological disorders like Alzheimer's and Parkinson's, as well as bone problems like osteomalacia (Doroszkiewicz *et al.,* 2023). Some studies suggest potential connections to other conditions, such as breast cancer and autoimmune issues, but the evidence is inconclusive (Hao *et al.,* 2022; Ungureanu and Mustatea, 2022). According to recent reports, the toxic effects of aluminum exposure have been linked to anemia in both people and animals (Cirovic and Cirovic, 2022). Additionally, it can lead to biochemical and metabolic abnormalities, resulting in tissue harm due to oxidative injury and contributing to disease development.

Oxidative redox components, i.e., reduced glutathione (GSH) and superoxide dismutase (SOD), are susceptible to damage caused by Al assault (Laabbar *et al.,* 2021). Lately, there has been an increasing interest in employing nanoparticles as adsorbents in the medium to address the phytotoxicity caused by heavy metals (Zhou *et al.,* 2020b). Tiny particles, i.e., nanoparticles, nanomembranes, and nano-powders, are being used in new ways to identify and remove harmful ingredients from water. These ingredients include heavy metals like aluminum, lead, mercury, copper, and unwanted chemicals like cyanide, nitrates, and organic pollutants (Mathur *et al.,* 2022; Praveen *et al.,* 2023).

Nanotechnology has been applied in water purification and supply systems, which has caught the interest of phytoremediation experts. Zinc oxide nanoparticles (ZnONPs) possess distinct optical and electrical characteristics that make them suitable for many applications, including developing coatings that may effectively eliminate harmful chemical and biological contaminants, including heavy metals (Sharifan *et al.,* 2020). After three days of treatment, the green Zn nanoparticles observed a reduction in the concentration of Pb and Cd heavy metals in contaminated water. As there are no available studies on the mitigation effect of ZnNPs on heavy metal accumulation in vivo, this study evaluated the biological activities of ZnNPs as antioxidant, anticancer, anti-alzheimer, antibacterial, and antiviral agents besides their impact on reducing the toxicity in aluminum-treated albino mice.

MATERIALS AND METHODS

Preparation of mycogenic zinc nanoparticles: Preparation of fungal extract: *Aspergillus fumigatus* was isolated from the soil. Ten grams of soil samples were stirred in 90mL of sterile saline solution for 15 min to obtain 10^{-1}. Serial dilutions were prepared until 10^{-7}. 100µL of each dilution was spread over potato dextrose agar (PDA) plates supplemented with different concentrations of zinc nitrate ($Zn(NO_3)_2$) (2, 4, and 6mM). The previous PDA plates were incubated at 28°C for 96h. The Zinc-tolerant fungus was selected and identified based on colonial and cultural features and the morphological characteristics of the sporangia and conidia using standard methods as described in the Pictorial Atlas of Soil and Seed Fungi by Montoya-Castrillón *et al.* (2021). Direct observation of colony features on PDA was used as a yardstick for colonial identification. Morphological features were observed under a high-powered imaging microscope on a slide preparation after staining with lactophenol cotton blue. Pure culture was maintained at 4°C on potato dextrose agar (PDA) slant until needed.

Spores from a 48-72 h-old culture of *Aspergillus fumigatus* cultivated aerobically in a 250 mL Erlenmeyer

flask containing a 100 mL potato dextrose broth (PDB; Sigma-Aldrich, USA). The flask was incubated in a shaking incubator (Labtron, Camberley, UK) at 30℃ and 2 ×g for 72h. The cultivation was conducted under ambient room lighting conditions without adding extra illumination, and fungal biomass ($2x10^3$) was harvested after cultivation. Ten grams of the fungal biomass was suspended in 100mL of sterile distilled water in an Erlenmeyer flask (250mL) and stirred at 4.5×g and 30℃ for 72h. The cells were discarded after filtration (using Whatman No.1 filter paper) to obtain an *Aspergillus fumigatus* bioactive filtrate (Mekky *et al.*, 2021).

Mycogenic *Synthesis of Zinc Nanoparticles:* Zinc NPs were synthesized using the filtrate of the fungus *Aspergillus fumigatus* obtained as described in the section above. 2.5 grams of $Zn(NO_3)_2$ was dissolved in 250 mL of deionized distilled water during biological synthesis. 100mL of $Zn(NO_3)_2$ were mixed with 100mL of *Aspergillus fumigatus* bioactive filtrate. Sodium hydroxide NaOH (0.1 M) was added in drops with constant stirring using a magnetic stirrer for an hour until the pH adjusted to 11. For three days, the solution was incubated in a shaking incubator (Labtron, Camberley, UK). A pale white solution of ZnO nanoparticles was obtained, as described by Shamim *et al.* (2019).

Characterization of the Zn nanoparticles: The physical properties of the synthesized nanoparticles were determined using the following devices. UV–Vis spectrophotometer (SPECORD 200 PLUS, Analytik Jena GmbH+Co. Jena, Germany) was used to confirm the synthesis. Transmission electron microscopy (TEM) (JEOL, USA) was used to determine the size of NPs. Zeta sizer and Zeta potential (Bettersize, USA) were used to determine the size and charge of nanoparticles (Abdel-Moneim *et al.*, 2022; Saad *et al.*, 2022).

The activities of mycogenic zinc nanoparticles:

Antioxidant activity: The DPPH scavenging activity of ZnNPs was estimated by Alowaiesh *et al.* (2023) with some modifications, 3 mL of an ethanol DPPH (Sigma, USA) added to 1 ml of the ZnNPs (25, 50, 75, 100 µg/ml). This mixture was then incubated in the dark for 30 min. The developing color was read at 517 nm using a spectrophotometer (SPECORD 200 PLUS, Analytik Jena GmbH+Co. Jena, Germany). The DPPH free radical was neutralized by the ZnNPs, indicating their antioxidant potential. The absorbance was applied in the following equation. The IC_{50} value presents the minimum concentration required to scavenge 50% of the DPPH radical (El-Saadony *et al.*, 2022).

$$\% \, DPPH \; scavenging \; activity = \frac{Abs \; control - Abs \; sample}{Abs \; control} \text{ x } 100$$

Anticancer activity: The monolayer of brain cancer cell lines U-87 MG (ATCC, USA) was trypsinized, and the cell count was adjusted to 1.0×10^5 cells/mL using DMEM media containing 10% fetal bovine serum (FBS). To each well of the 96-well microtiter plate, 100 µL of the diluted cell suspension (1×10^4 cells/well) was added. The microtiter plate was incubated at 37°C in CO_2 conditions for a day. The medium was replaced with a fresh one supplemented with FBS and varying concentrations of ZnNPs (25, 50, 75, 100 µg/ mL), then incubated for two days at 37°C. The cells were harvested using a trypsin-EDTA buffer and treated with trypan blue to distinguish the viable cells. The live cell count was determined, and the results were presented as the percentage of inhibition of brain cancer cell lines (Olivares-Bañuelos *et al*., 2019).

Antibacterial activity: *Streptococcus pyogenes* (SP) *Staphylococcus aureus* (SA), *Listeria monocytogenes* (LM), *Bacillus cereus* (BC), *Escherichia coli* (EC), *Klebsiella pneumoniae* (KP), and *Salmonella* Typhi (ST) were used to measure the antibacterial activity of ZnNPs. The bacterial strains were kept at 4°C by subculturing them on nutrient agar slants. El-Saadony *et al.* (2021b) used the agar well-disc-diffusion method to assess the bactericidal activity of ZnNPs. After adding 50mL of melted Muller-Hinton agar (MHA) to plates, 0.1mL of bacterial inoculum (1.5×10^8 CFU/mL) was spread on the hardened MHA. Each plate (9 cm) was punched with 8mm wells and introduced 6 mm discs saturated with 50µL ZnNPs levels (25, 50, 75, and 100 µg/mL). For 24–48h, MHA plates were incubated at 37°C (El-Saadony *et al.*, 2019). Diameters of the resulting inhibition zones (mm) indicated the antibacterial activity (El-Saadony *et al.*, 2021a). The MIC was estimated as the method described by Saad *et al.* (2021).

Antiviral activity of ZnNPs:

Virological samples*:* Five skin nodule samples were collected from suspected cattle showing the clinical signs of lumpy skin disease (LSD) (such as fever and nodules on the skin). These samples were labeled, transported, and stored at -80 ºC according to OIE (2010) until be used for real-time PCR (Stratagene Mx3005P, Agilent, USA), isolation, sequencing, and application of antiviral nanomaterials.

Real-time PCR for detection of LSDV: The five skin nodule samples were examined by real-time PCR. The viral DNA was extracted from suspected prepared samples using (G-SPIN™ Total DNA Extraction Kit, Korea) according to the manufacturer's instructions and stored at -20°C. The mix kit (LSDV dtec-qPCR test (GPS, Spain) was applied to a real-time PCR machine (Stratagene Mx3005P, Agilent, USA). The reaction was prepared in a sterile 0.2mL tube. 20µL qPCR mix was prepared and mixed thoroughly with 4µL mix stable qPCR 5x, 1µL specific primer/probe, 10µL DNase/RNase free water, and 5µL template (either sample, positive or negative). The thermal profile, as described by the manufacturer of the mixing kit, was adjusted to one cycle at 95°C for 15min for (activation), followed by 40 cycles at 95°C for 15sec for (denaturation) and 60°C for 1min for (hybridization/extension and data collection). The cut-off was at 35 cycle threshold (Ct) value as determined by the manufacturer (Zeedan *et al.*, 2019).

Isolation of LSDV on CAM of SPF-ECEs: One positive skin nodule sample was selected to be isolated on the chorioallantoic membrane (CAM) of a specific pathogen-free- embryonated chicken egg (SPF-ECE) (House *et al.*, 1990). The sample was prepared in phosphate-buffered

saline (pH 7.4) with 100 U/mL penicillin and 100 mg/mL streptomycin. The homogenate was frozen and thawed trice to lyse the cells, then the supernatant was purified by centrifuging at 6000×g for five minutes at 4°C, then filtered through a 0.45 mm pore-size cellulose acetate filter. Before inoculation, the SPF-ECEs were incubated for nine days at 37°C and 70% humidity. Then, they were injected with 0.2 mL of the supernatant through CAM after being incubated for 9 days (Schneiderhan *et al.,* 2007). Every day for seven days following inoculation, the ECEs were examined, and eggs that had died embryos within the first 24 hours after inoculation were regarded as non-specific deaths. Three virus passages in CAM were done to increase the virus titer. The application of conventional PCR confirmed the result.

Antiviral activity of ZnONPs against LSDV: The IC_{50} of ZnONPs against LSDV was determined following previously established protocols (AbouAitah *et al.,* 2021) using Ribavirin as a reference antiviral compound for comparison (Gupta *et al.,* 2022). In each 96-well tissue culture plate well, 100 µL of Madin-Darby bovine kidney (MDBK, European Collection of Authenticated Cell Cultures (Public Health England) cell suspension (3×10^5 cells) was added and incubated overnight in a humidified incubator at 37°C with 5% CO_2. These cells are necessary for propagating and studying the bovine poxvirus LSDV. The cell monolayers were washed once with 1x Phosphate-buffered saline (PBS, Sigma, USA) and then subjected to LSDV adsorption for 1 hour at ambient temperature (25 °C). The cell monolayers were overlaid with 50 µL of Modified Eagle's Medium (DMEM; Life Technologies) containing varying concentrations of ZnONPs or Ribavirin. After incubating for 72h at 37 °C in 5% CO_2, the cells were stained with 0.1% crystal violet in distilled water for 15 min at room temperature after being fixed with 100µL of 4% paraformaldehyde (Sigma, USA) for 20 min. The optical density of the color was then determined at 570nm using an Anthos plate reader (BMGLABTECH®FLUOstar Omega, Germany) after the crystal violet dye had been dissolved using 100µL of absolute methanol per well. Using GraphPad Prism software (version 5.01) and nonlinear regression analysis, the IC_{50} value was determined by plotting the logs of the concentrations of ZnNPs and Ribavirin against the normalized response (variable slope) (Homaeigohar *et al.,* 2023).

Anticholinesterase activity (Anti-Alzhamir) of mycogenic Zinc nanoparticles: The acetylcholinesterase activity was evaluated using an enhanced Ellman technique, utilizing a Quanti-Chrome assay kit (USA) in a 96-well plate reader (BMGLABTECH®FLUOstar Omega, Germany). The enzyme catalyzes the hydrolysis of the substrate acetylthiocholine, yielding the product thiocholine, then undergoes a reaction with 5,5-dithiobis (2-nitrobenzoic acid) (DTNB), resulting in the formation of DMNB-5-MNBA and 5-thio-2-nitrobenzoate, which exhibits a yellow color. The chromogen yellow color's intensity and absorbance may be measured at 412nm, directly related to the enzyme activity in the examined materials (El-Hawwary *et al.*, 2021).

Experimental layout, Basal diet: A total of 120 mice weighing (30-42g) were obtained from the breeding animal house, adapted, and kept under full hygienic conditions. The plastic boxes were subjected to a 12h dark-light cycle, 40–60 % relative humidity, and a temperature of 23.2ºC. The mice delivered water and diet throughout the experiment (NRC, 1994). The mice were given basal diet for two weeks to acclimate to the experimental animal laboratory setting. The accommodation and administration of the animals and the experimental protocols were conducted per the principles delineated in the Guide for the Care & Use of Lab Animals following the National Committee of Bioethics (NCBE 2023). Randomly, ten mice were allocated to six groups: Group 1 (Control) received a basal diet with no additives; Group 2: fed the control diet supplemented with 25 mg/kg of zinc nanoparticles (ZnNPs); Group 3: Fed the control diet supplemented with 50 mg/kg of ZnNPs; Group 4: Fed the control diet supplemented with 75 mg/kg of ZnNPs; Groups 5: $AlCl_3$-challenged chicks that were fed a basal diet; Group 6: $AlCl_3$-challenged quails fed a control diet supported with 75 mg/kg ZnNPs. Aluminum chloride solution was prepared and added to water with a 100 mg/kg concentration bw/day for 30 days (Gomaa *et al.,* 2019).

Growth performance: At the end of the experiment, the animals were decapitated from the cervical region. Following the dissection of the heart, brain, liver, kidney, lung, and spleen, excess fat was eliminated, & the percentages of the relative weight of organs were calculated (Zhou *et al.*, 2024).

Blood biochemistry: The biochemical parameters were following ways: ALT, AST, Urea, Creatinine (Spectrum, Egypt, Cat no. # 216 001), and creatine kinase (CK) activities (Spectrum, Egypt, Cat no. # 238 001) were determined in serum (Moss, 1982; Burtis and Ashwood, 1999) respectively. Antioxidant parameters: estimation of malondialdehyde (MDA), superoxide dismutase (SOD), catalase (CAT), and glutathione peroxidase (GPx) were determined via utilizing commercial kits (Biodiagnostic, Egypt) (Aftab *et al.*, 2018; Al-Hazmi *et al.*, 2021).

Proinflammatory and Proapoptotic markers: The Gene analysis was conducted with real-time PCR, and RNA was isolated from the tissue with Trizol (Invitrogen; Thermo Fisher Scientific, Inc.) as mentioned by Khamis *et al.* (2023). For evaluating the RNA quality, the A260/A280 ratio was analyzed by applying the NanoDrop® ND–1000 Spectrophotometer (NanoDrop Technologies; Wilmington, Delaware, United States) for 1.5µL of the RNA. A High-Capacity cDNA Reverse Transcription Kit cDNA Kit (Applied Biosystems™, USA) was used for cDNA synthesis. The RT reaction mixture was kept for 60 min at 45°C, subsequently by 10 min at 85°C to inhibit the enzyme in a Biometra 96-well thermal cycler (Applied Biosystems).

The expression level of the target genes was normalized by applying the mRNA expression of a known housekeeping gene, B-actin. Data are presented as fold-changes compared to the control group following the $2^{-\Delta\Delta CT}$ method (Rao *et al.*, 2013).

Histology: Carcass tissues (brain, liver, and kidney) were picked, preserved in formalin, and processed by an automated processor. The initial phase was fixed and then dehydrated. The fixation was conducted by immersing the tissue for 48h in 10% formalin, after which the fixation solution was removed using distilled water for 30min. The tissues were subsequently dehydrated by immersing in elevating levels of alcohol (70, 90, and 100%) for 120 min in 70% alcohol then 90min in 90%. The dehydration was subsequently cleared using multiple cycles of xylene. The procedure involved submerging the tissue for one hour in a solution of 50% xylene & 50% alcohol and then for an additional 1.5h in pure xylene. The specimens were then saturated with melted paraffin wax, encased, and sealed. Hematoxylin & eosin were used for 4-5µm paraffin cut sections (Suvarna and Niranjan, 2013). Blood circulation disruptions, irritation, degenerations, apoptosis, necrosis & additional histopathological alterations in the tissues were monitored.

Statistical analysis: The triplicate data were presented as mean ±SE and statistically analyzed by one-way ANOVA. The data were compared for significant differences using the LSD test at $P<0.05$. The statistical analysis was conducted using SPSS (IBM, USA).

RESULTS

Characterization of Zinc nanoparticles fabricated by *Aspergillus fumigatus*: This study used the *Aspergillus fumigatus* strain to synthesize myogenic ZnNPs, proving its efficiency in reducing zinc nitrate from colorless to white. The morphological properties of *Aspergillus fumigatus* were colony size 200-400; stripes color was grayish; the colony surface was smooth walled; vesicle serration was uniseriate pyriform; metula covering was upper 2/3, the shape was globose small in columns and smooth conidia surface.

The biomass of *Aspergillus fumigatus* efficiently converted zinc nitrate into zinc nanoparticles, exhibiting a color change from colorless to white. The ZnNPs exhibited absorption of UV light at a wavelength of 350 nm (Fig. 1A). They possessed a spherical form (Fig. 1B), with a median diameter of 39 nm, as determined by zeta sizer analysis. Additionally, they carried a negative charge of 23.6 mV as determined by zeta potential analysis (Fig. 1C, 1D).

***In vitro* ZnNPs activities:**

Antioxidant activity of ZnNPs: The zinc nanoparticles have considerable ($P<0.05$) scavenging activity against DPPH free radicals. The findings demonstrated a positive correlation between the concentration of ZnNPs and its antioxidant activity. The ZnNPs at the maximum concentration (100 µg/mL) eliminated 89% of DPPH radicals. The IC_{50} value represents the minimum concentration required to scavenge 50% of the free radicals; in this study, it was 20 µg/mL (Fig. 2).

Anticancer activity of ZnNPs: ZnNPs concentrations have considerable anti-tumor activity against U-87 MG brain cancer cell lines. The ZnNPs concentrations gradually inhibited the brain cancer cell progress (Fig. 3 A, B, C, D), where ZnNPs (100 µg/mL) significantly reduced 85% of cancerous cells compared to Doxorubcin (Fig. 3F). The IC_{50} of ZnNPs was (50 µg/mL), successfully inhibiting 50% of cancerous cells.

Antibacterial activity of ZnNPs: Zinc nanoparticles' concentrations (25, 50, 75, and 100 µg/mL) have significant antibacterial activity ($P<0.05$) against pathogenic bacteria (*Streptococcus pyogenes*, *Staphylococcus aureus*, *Listeria monocytogenes*, *Escherichia coli*, and *Salmonella* Typhi, *Klebsiella pneumoniae*). The inhibition zones' diameters increased in a concentration-dependent manner. *S. aureus* showed the most sensitivity to ZnNPs (100 µg/mL), with an inhibition zone diameter (IZD) of 33 mm. *S. pyogenes* had a slightly lower sensitivity with an IZD of 32 mm. On the other hand, *Salmonella Typhi* exhibited the highest resistance to ZnNPs (21 mm), followed by *Klebsiella pneumoniae* (22mm). The MIC values of ZnNPs against tested bacteria ranged from 10-25 µg/mL as depicted in Fig. 4.

Antiviral activity of ZnNPs: Mycogenic synthesized ZnONPs reduced 88% of the lumpy skin disease virus (LSDV) compared to 90% of Ribavirin. ZnNPs have IC_{50} of 35.66 µg/mL against LSDV while they have IC_{50} of 25.12 µg/mL on MDBK tissue culture, while Ribavirin has IC_{50} of 29.89 µg/mL against LSDV while it has IC_{50} of 18.78 µg/mL on MDBK tissue culture as described in Fig. 5.

Alzheimer activity of ZnNPs: This study aimed to assess mycogenic ZnNPs' *in vitro* inhibitory effect on the acetylcholinesterase enzyme (AChE) associated with alzheimer's disease. The results were then compared to the inhibitory activity of the conventional AChE inhibitor medicine, donepezil. The results showed that Zn nanoparticles synthesized using *Aspergillus fumigatus* (100 µg/mL) showed the highest and most promising anti-acetylcholinesterase activity, where 84% of AChE activity was inhibited with no sense with donepezil. The IC_{50} values were 51.32 µg/mL for ZnNPs and 56.11 µg/mL for donepezil, as shown in Fig. 6.

Growth incidences: Different treatments of ZnNPs gradually raise the weight gain, which reaches the maximum at 75 ppm (83.6g) with a relative increase of 27 and 62% over the control and $AlCl_3$-challenged groups, respectively (Table 1). The challenged group recorded the lowest weights in mice (51.3g). Adding ZnNPs to the challenged mice's diet significantly enhanced the WG to 58.7g. The high FCR explains this increase in BWG in ZnNP-treated groups (1.57) compared to (1.35) in the $AlCl_3$-infected group, which is regulated with the ZnNPs additions. The relative organ weight showed the highest values in the challenged group (4.1g), which recovered with ZnNPs into 2.9g. No death was observed in all treatments. From the results in Table 1, the supplementation of ZnNPs considerably enhances the growth performance parameters and mitigates the adverse effects of $AlCl_3$.

Blood biochemistry: Table 2 shows the blood chemistry of the $AlCl_3$-challenged mice and the effect of ZnNPs on mitigating the Al toxicity. The liver enzyme activity considerably increased in the $AlCl_3$-challenged group (310 and 256 U/l for ALT and AST, respectively); however, adding

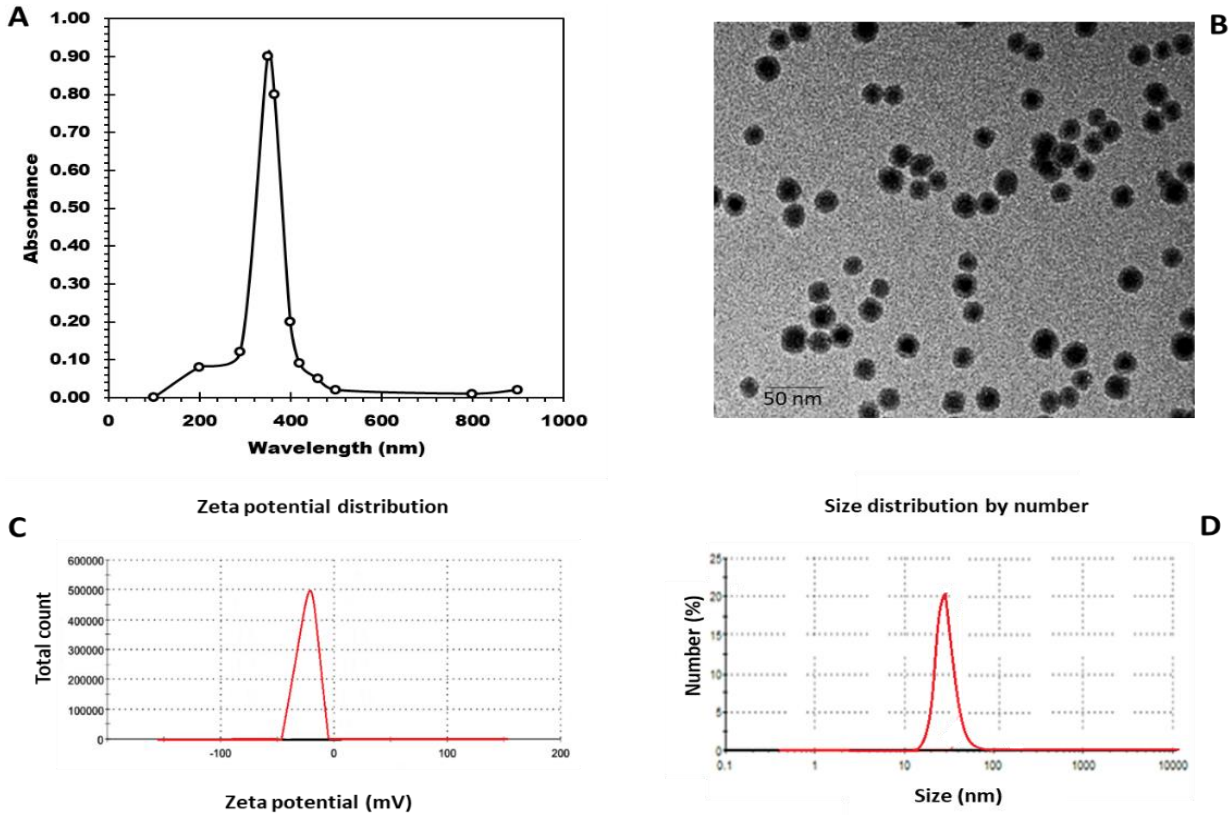

Fig. 1: Characterization of biological zinc nanoparticles fabricated by *Aspergillus fumigatus* (A), UV absorbance at 350nm, (B) average size of 31-70nm, (C) negative charge of -23.6mV, (D) Size of zinc nanoparticles of 39nm.

Table 1: Effect of dietary treatments ZnNPs on growth performance Parameters of $AlCl_3$-challenged mice.

Parameters	Control	T1	T2	T3	T4	T5	p-value
LBW (g)	30.1±0.0	32±0.1	32±0.5	31±0.2	30±0.2	31±0.0	0.89
FBW (g)	95.6±0.9c	105.4±0.9bc	110.3±2.2b	114.6±1.0a	81.3±1.5e	89.7±2.1d	<0.0001
BWG (g)	65.6±0.2c	73.4±1.1b	78.3±1.6b	83.6±1.0a	51.3±0.9e	58.7±1.9d	<0.0001
FCR	1.42±0.1bc	1.46±0.2b	1.51±0.5ab	1.57±0.1a	1.35±0.6d	1.40±0.2c	0.04
SR	100	100	100	100	100	100	0.9
ROW	2.46±0.1d	2.49±0.2cd	2.52±0.1c	2.54±0.2c	4.1±0.8a	2.9±0.2b	0.036

Data are presented mean ±SE. Significant differences in the same raw were indicated by different lower cases (a-e) at $p<0.05$ using LSD. Control was delivered basal diet; T1, control diet supplemented with 25 mg/kg ZnNPs; T2 control+50 mg/kg ZnNPs; T3 control+75 mg/kg ZnNPs; T4, $AlCl_3$-challenged mice; T5, AlCl3-challenged mice and treated with ZnNPs (75 mg/kg). Live body weight (LBW); Final body weight (FBW); weight gain (BWG), Feed intake (FI), Feed conversion ratio (FCR), survival rate (GR), and relative organ weight (ROW).

ZnNPs to the challenged group diet regulated the enzyme activity with relative decreases of 53 and 46%, respectively. The uric acid recorded the highest values in T4 (7.2 mg/dl), which decreased by 32% in T5. The dietary ZnNPs significantly enhanced the lipid profile, where their levels in T3 were 50, 15, and 55 mg/dl for TC, LDL, and HDL.

On the other hand, the $AlCl_3$-challenged group showed higher TC and LDL and lower HDL, but ZnNPs regulated these levels. Adding ZnNPs to mice, diet enhanced the oxidative stability in the $AlCl_3$-challenged group, where decreased MDA and enhanced the activity of the enzymatic defense system (SOD, CAT, and GPx).

Proinflammatory and proapoptotic markers: The impact of dietary ZnNPs on the relative expression of the intestinal health markers (OCCU and MUC-1) in $AlCl_3$-challenged mice is shown in Table 3. The gene expression of OCCU and MUC-1 genes appeared normal in the control, T1, T2, and T3, reflecting the intestinal health. At the same time, T4 reveals a huge upregulation in the genes of these markers. The addition of ZnNPs downregulated the gene expression by 55%.

The impact of ZnNPs supplementation on the relative expression of the liver and renal inflammatory (IL-6 and IL-1β) and precancerous (Bax and caspase-3) markers in $AlCl_3$-challenged mice were expressed in Table 3. The expression of renal inflammatory markers and precancerous markers were regular in control, T1, T2, and T3; conversely, they revealed a significant rise in T4. The mice in T5 revealed a considerable improvement in the expression of the liver and renal inflammatory (IL-6, IL-1β) and precancerous (Bax and caspase-3) markers compared to T4.

Histological observation: The liver sections of control mice and ZnNPs-fed mice (25, 50, and 75 mg/kg) showed normal hepatic central vein and hepatic cords and typical histological structure of hepatic lobule (Fig. 7IA, B, C, D), the $AlCl_3$-challenged mice showed perivascular collagen fibers deposits (star) adjacent severe acute cell swelling and focal hepatic necrosis (Fig. 7IE). The ZnNPs treatment (75 mg/kg) in $AlCl_3$-challenged mice showed normal liver tissue structure recovery with mild peribiliary lymphocytic infiltrations (Fig. 7IF).

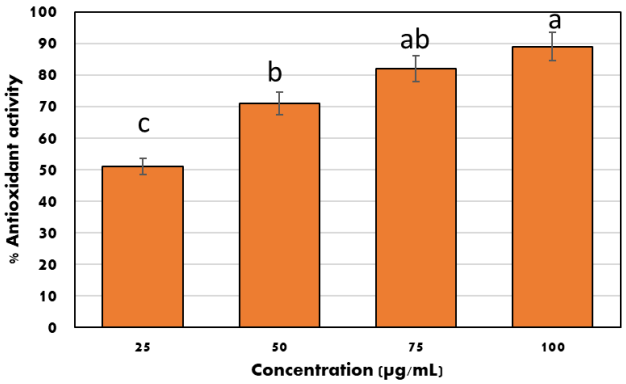

Fig. 2: Antioxidant activity of ZnNPs fabricated by *Aspergillus fumigatus* against DPPH free radicals. The significant differences between concentrations are indicated by lowercase letters (a-c) above columns at P<0.05.

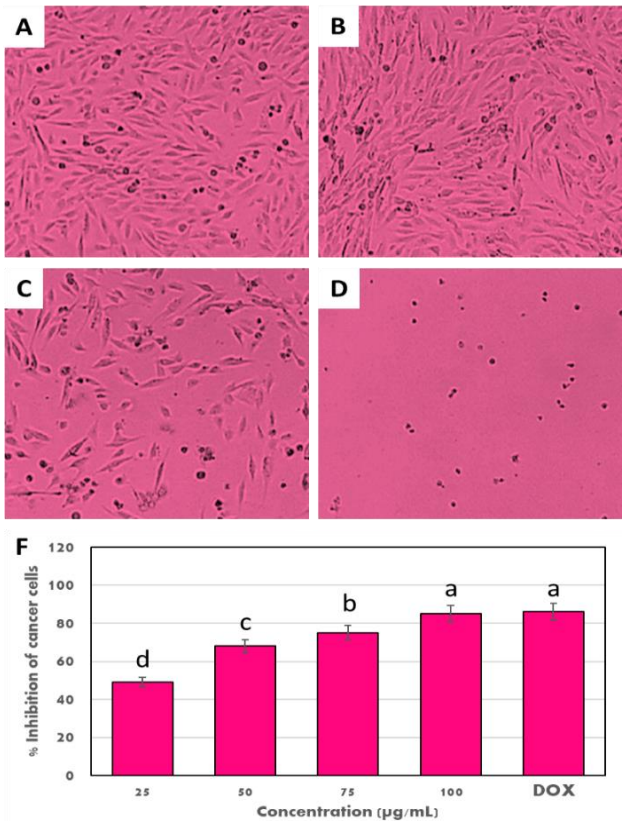

Fig. 3: Cytotoxicity of ZnNPs fabricated by *Aspergillus fumigatus* against brain cancer cell lines. (A) control brain cancer cell lines, (B) the inhibitory effect of ZnNPs (50 µg/ mL) on brain cancer cell lines, (C) the inhibitory effect of ZnNPs (75 µg/mL) on brain cancer cell lines, (D) the inhibitory effect of ZnNPs (100 µg/ mL) on brain cancer cell lines, (F) The % inhibition of brain cancer cell lines of ZnNPs concentrations compared to Doxorubcin.

On the other hand, kidney sections showed normal renal parenchyma and typical renal architectures in control and ZnNPs-fed mice (25, 50, and 75 mg/kg) (Fig. 7II A, B, C, D), the $AlCl_3$-challenged mice showed hypertrophied blood vessels in pelvic region which vacuolated media, interstitial, perivascular inflammatory edema and an adjacent large area of necrotic tubules (Fig. 7IIE) while the $AlCl_3$-challenged mice and treated with ZnNPs (75 mg/kg) showed standard renal architectures with mild perivascular edema (Fig. 7IIF), indicating the mitigative effect against the Al toxicity on kidney.

The brain histology sections are presented in Fig. 7III. The control groups and ZnNPs-fed mice (25, 50, and 75 mg/kg) showed normal brain tissue (Fig. 7III A, B, C, D), the Al toxicity caused prominent perivascular edema (star) with a little dark degenerated neuron (Fig. 7IIIE), meanwhile the $AlCl_3$-challenged mice and treated with ZnNPs (75 mg/kg) showed normal brain tissues with mild perivascular edema, mild demyelination (Fig. 7IIIF).

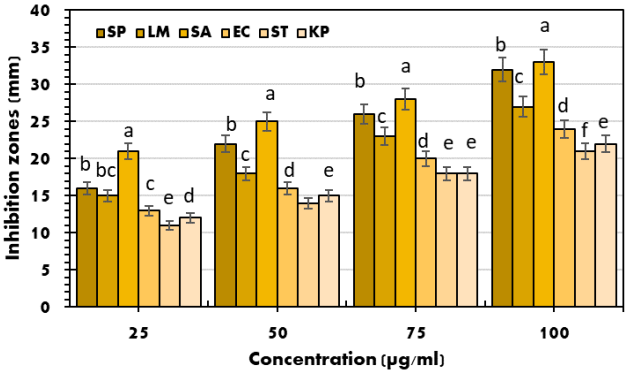

Fig. 4: Antibacterial activity of ZnNPs fabricated by *Aspergillus fumigatus* against pathogenic bacteria *Streptococcus pyogenes* (SP), *Listeria monocytogenes* (LM), *Staphylococcus aureus* (SA), *Escherichia coli* (EC), *Salmonella* Typhi (ST) and *Klebsiella pneumoniae* (KP). The significant differences between samples are indicated by lowercase letters (a-f) above columns at P<0.05.

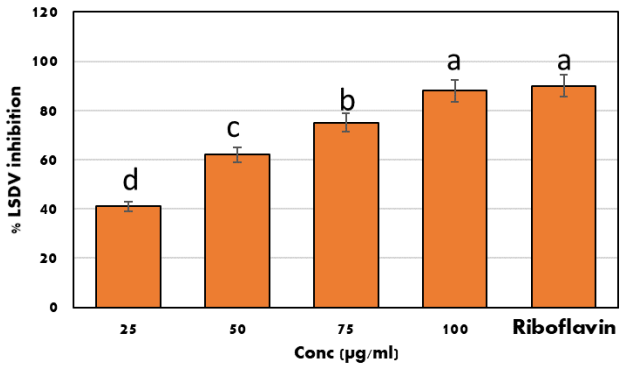

Fig. 5: *In vitro* antiviral activity of ZnNPs fabricated by *Aspergillus fumigatus* against LSDV activity. The significant differences between samples are indicated by lowercase letters (a-d) above columns at P<0.05.

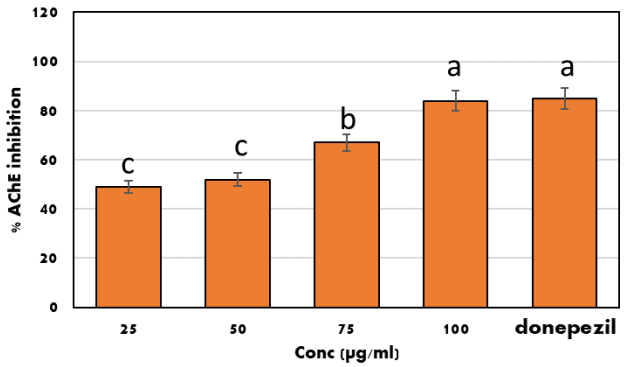

Fig. 6: *In vitro* anticholinesterase activity of ZnNPs fabricated by *Aspergillus fumigatus* against AChE activity. The significant differences between samples are indicated by lowercase letters (a-c) above columns at p<0.05.

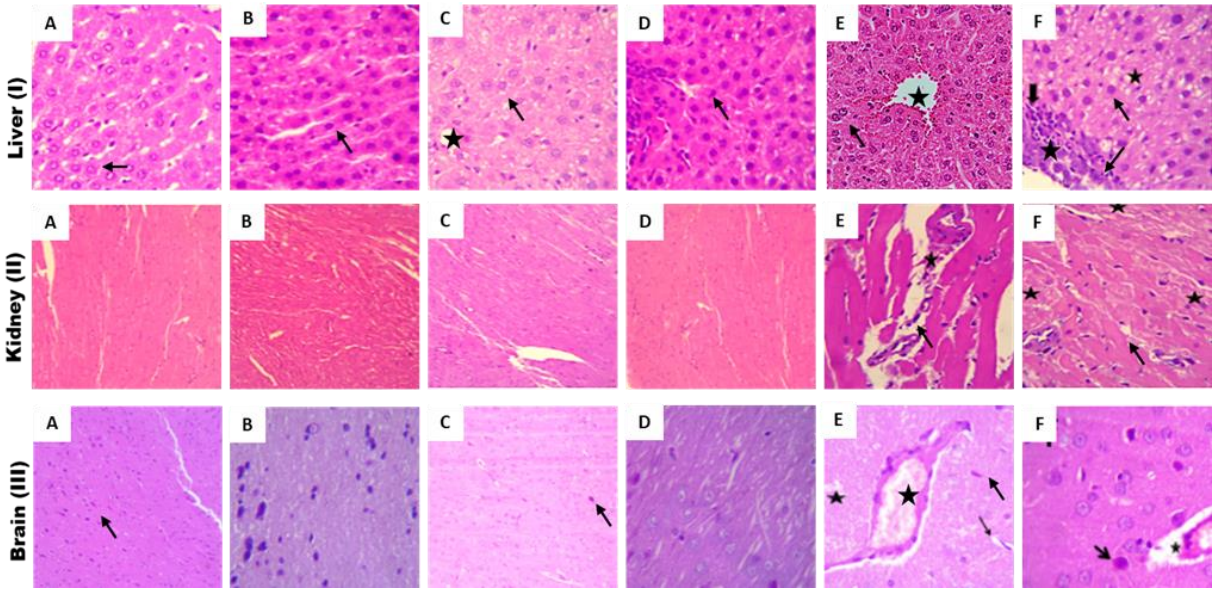

Fig. 7: Photograph of liver sections stained by H&E, magnification power (100X). (A, B, C, and D) control and three mice groups delivered 25, 50, and 75 mg/kg of ZnNPs showed normal liver structure as control, E) $AlCl_3$-challenged mice showed perivascular collagen fibers deposits (star) adjacent severe acute cell swelling, and F) showed the mitigating effect of ZnNPs 75 mg/kg on aluminum toxicity by the gradual recovery of the normal liver tissues. Photograph of kidney sections stained by H&E, magnification power (100X). (A, B, C, and D) control and three mice groups delivered 25, 50, and 75 mg/kg of ZnNPs showed normal kidney histological structure as control, E) AlCl3-challenged mice showed interstitial, perivascular inflammatory edema (star) an adjacent large area of necrotic tubules, and F) showed the mitigating effect of ZnNPs 75 mg/kg on aluminum toxicity by the gradual recovery of the normal kidney tissues. Photograph of brain sections stained by H&E, magnification power (100X). (A, B, C, and D) control and three mice groups delivered 25, 50, and 75 mg/kg of ZnNPs showed normal cardiomyocyte fibers with mild intramuscular congested blood vessels, E) AlCl3-challenged mice showed degeneration of cardiomyocytes mainly hydropic degeneration, and F) showed the mitigating effect of ZnNPs 75 mg/kg on aluminum toxicity by the gradual recovery of the normal brain tissues.

Table 2: Effect of dietary treatments ZnNPs on serum kidney and liver function, lipid profile and immunity parameters of $AlCl_3$-challenged mice.

Serum parameters	Treatments (mg/kg)						P value
	Control	T1	T2	T3	T4	T5	
Liver and Kidney functions							
AST (U/L)	125±2.1a	115±3.0b	112±3.0c	109±1.9e	256±3.2	119±1.2d	<0.0001
ALT (U/L)	160±0.2a	156±0.2b	150±0.2c	142±0.1d	310±0.1	165±0.1c	<0.0001
Creat. (mg/dL)	0.33±0.01	0.34±0.02	0.35±0.01	0.31±0.00	0.36±0.02	0.32±0.01	0.99
Uric acid (mg/dL)	5.6±0.3a	4.6±0.6b	4.2±0.2c	3.5±0.3d	7.2±0.5	4.9±0.5c	0.001
Lipid profile							
TC (mg/dL)	75±1.1a	69±0.8b	61±1.2b	50±1.8d	125±1.1	65±1.5c	<0.0001
LDL (mg/dL)	20±0.2a	18±0.4b	17±0.8c	15±0.2d	50±0.6	22±0.8c	0.001
HDL (mg/dL)	36±0.6c	42±0.8b	49±0.7b	55±1.1a	25±0.8	35±0.5b	0.001
Abdominal fat	1.2±0.1a	1.0±0.2ab	0.85±0.01b	0.70±0.0c	1.45±0.2	0.79±0.01b	0.001
Antioxidant status							
MDA (nmol/mL)	2.1±0.5	1.5±0.3	0.89±0.03	0.31±0.02	4.8±0.2	2.8±0.3	<0.0001
SOD (U/mL)	3.5±0.6	4.2±0.5	5.1±0.9	6.2±0.5	2.1±0.2	4.4±0.5	<0.0001
CAT (U/mL)	5.2±0.3	5.6±0.6	6.3±0.3	7.6±0.5	4.2±0.3	5.9±0.2	<0.0001
GPx (U /mL)	25±0.1	29±0.2	33±0.3	35±0.1	12±0.1	21±0.1	<0.0001

Aspartate Aminotransferase (AST), Alanine Transaminase (ALT), Creatinine (Create.), Total cholesterol (TC), low density lipoprotein (LDL), High density lipoprotein (HDL), Immunoglobin G (IgG), Immunoglobin A (IgA), Malondialdehyde (MDA), superoxide dismutase (SOD), Catalase (CAT), Peroxidase (GPx). Data are presented mean ±SE, Significant differences in the same raw were indicated by different lower cases (a-e) at $p<0.05$ using LSD. Control was delivered basal diet; T1, control diet supported with 25 mg/kg ZnNPs; T2 control+ 50 mg/kg ZnNPs; T3 control+ 75 mg/kg ZnNPs; T4, $AlCl_3$-challenged mice; T5, $AlCl_3$-challenged mice and treated with ZnNPs (75 mg/kg).

Table 3: The effect of dietary ZnNPs on the relative expression of the proinflammatory cytokines (OCCU and MUC-1, IL-1β, IL-6), and precancerous markers (BAX and Casp-3) in $AlCl_3$-challenged mice.

Genes	Proinflammatory markers				Precancerous markers	
	OCCU	MUC-1	IL-1β	IL-6	BAX	Casp-3
Control	1±0.01ab	1.1±0.02ab	1.1±0.03e	1±0.3d	1±0.2e	1.04±0.1e
T1	0.5±0.02b	0.6±0.01b	2.1±0.2c	1.6±0.3c	2.5±0.1c	1.8±0.2c
T2	0.3±0.01c	0.4±0.03b	1.6±0.1d	1.3±0.2cd	1.7±0.2d	1.4±0.5d
T3	0.12±0.03d	0.16±0.01c	1.3±0.2de	1.1±0.1d	1.3±0.1e	1.2±0.2e
T4	1.3±0.1a	1.5±0.2a	10±0.9a	9.8±0.8a	13±0.7a	7.8±0.9a
T5	0.61±0.02b	0.7±0.02b	4.2±0.5b	3.8±0.2b	5.2±0.2b	2.9±0.2b

Control was fed basal diet; T1, control+25 mg/kg ZnNPs; T2 control+50 mg/kg ZnNPs; T3 control+75 mg/kg ZnNPs; T4, $AlCl_3$-challenged mice; T5, $AlCl_3$-challenged mice and treated with ZnNPs (75 mg/kg).

DISCUSSION

Stress impacts many body parts and generates various physiological changes, which appear as symptoms including headache, nausea, heartburn, and exhaustion (Moustafa and Arisha, 2020). Stress has severe and enduring adverse effects that affect the animal's growth rate, feed intake, body weight, libido, and productivity (Al-Amin *et al.*, 2016). Acute and chronic stress can be

classified depending on how long it lasts. Both acute and chronic stress induce known physiological and biological problems, in particular, because of their substantial influence on the generation of reactive oxygen species (ROS) (Bosnjak *et al.*, 2019).

The anterior pituitary releases adrenocorticotrophic hormone (ACTH) in response to stress, and the hypothalamus then releases corticotropin-releasing hormone (CRH), which ultimately causes an increase in the synthesis and release of corticosteroids, including corticosterone (CORT), in rats. Different stress reactions are triggered in tissues upon CORT release, which negatively affects the production of CRH and ACTH from the brain and pituitary glands (Dinse. External stimuli, including heat, shock, noise, radiation, hyperoxia, toxins, and physical activity, increase the formation of free radicals (ROS). Normal cells create modest amounts of ROS, but their accumulation can disrupt macromolecules, including lipids, proteins, carbohydrates, and DNA structures (Arisha *et al.*, 2019). Thus, improving the antioxidant defenses is an effective therapeutic strategy for preventing free radical production and oxidative damage (Seyfi *et al.*, 2020).

In this study, Al caused oxidative stress in albino mice, and the efficacy of ZnO-NPs in mitigating $AlCl_3$ toxicity was evaluated. The high exposure to $AlCl_3$ in mice induced neurological disease symptoms like Alzheimer's disease (AD). The most distinctive alteration in AD is the elevation in acetylcholinesterase enzyme (AChE) inhibitory activity. AChE is the enzyme that breaks down acetylcholine in the brain, produced by cholinergic and non-cholinergic neurons (El-Saadony *et al*., 2023). Inhibiting AChE can raise acetylcholine levels, which may be beneficial in treating AD. The previous findings suggest that the selected extracts have a significant ability to combat AD. This property is attributed to active compounds on the nanoparticle surfaces, which can effectively treat Alzheimer's disease. These compounds can also help prevent the progression of AD by improving cognitive function in various animal models (Bakhtiari *et al.*, 2017; Bakoyiannis *et al.*, 2019).

Furthermore, the findings indicated that ZnO nanoparticles manufactured using green methods exhibited the highest level of acetylcholinesterase inhibitory action, possibly attributable to the large and reactive surface area.

Zn nanoparticles have been effectively utilized as vehicles for delivering medications to specific locations, decreasing undesired harmfulness and off-target effects and ultimately enhancing the combined benefits of the treatments (Mishra *et al.*, 2017). These treatments have the potential to be productive and beneficial in the management of alzheimer's disease. Additional research should be conducted in living organisms to elucidate the precise mechanism of inhibitory effect.

ZnO-NPs receive more attention in commercial and biomedical applications due to their antibacterial, anti-inflammation, anticancer, anti-diabetic actions, increased surface reactive area, bioavailability, and absorbability (Jiang *et al.*, 2018). ZnONPs have antiviral effects against several DNA and RNA viruses, such as Bovine herpes virus 1 (Zeedan *et al.*, 2020), influenza virus (H1N1) (Ghaffari *et al.*, 2019), and hepatitis viruses (Gupta *et al.*, 2022). The superiority and enhanced performance of ZnONPs compared to other antiviral metal oxide NPs can be attributed to their favorable compatibility with biological systems, affordability, high safety, and stability (Jiang *et al.*, 2018).

Our study demonstrated the antiviral effect of ZnONPs against LSDV at a concentration of 35.66 µg/mL. To the best of our knowledge, this is the first investigation to uncover the impact of green synthesized NPs on LSDV as a DNA virus. Antiviral activity of metal-based nanoparticles depends on three mechanisms: (A) adhering to the virus and preventing it from attaching to and entering the cell; (B) destruction of the structure of viral proteins and function of viral nucleic acids due to the production of highly active oxygen and other ions and radicals that stick to the wall (spikes or membrane); and (C) emulating the nucleus to boost the host cell's immune response and prevent the virus from budding and spreading (Zhou *et al.*, 2020a).

ZnONPs' remarkable antimicrobial properties can be attributed to their increased specific surface area because the smaller particle size increases the reactivity of the particle surface (Hassan *et al.*, 2022). Additionally, zinc ions selectively inhibit viral DNA polymerase, which prevents viral replication (Gupta *et al.*, 2022).

Bami *et al.* (2022) investigated the potential of nano-ZnO as a significant feed additive. The study found that supplementing diets with nano-ZnO ppm diet led to positive changes in the intestinal structure. Specifically, all sections of the small intestine in the nano-ZnO diet showed a significant increase in villus height, surface area, and total goblet cell count. These birds' villus height to crypt depth ratio was significantly higher, indicating improved intestinal health. Bahrampour *et al.* (2021) proposed that the improved zinc absorption from the nanoparticles might cause increased villus height. This enhanced bioavailability of Zinc could help maintain the health and function of the intestinal lining, which acts as a barrier against harmful substances. Another reason for a greater villus height in the gut segment could be that acidic mucin resists bacterial degradation, resulting in less cellular damage (Skalny *et al.*, 2021).

Furthermore, crypt evolution is required to increase the gut's cell renewal and maturation rate. The groups that received medication had significant growth improvement, as seen by lower ratings for intestinal lesions, indicating enhanced gut health. In addition, El-Katcha *et al.* (2018) found that zinc nanoparticles were more efficient than bulk zinc oxide, improving the growth markers. This is likely because Zn is a vital element for many enzymes in the body involved in metabolism. Consequently, ZnO-NPs may exhibit supplementary actions that enhance development.

The present investigation demonstrated a substantial elevation of liver markers in the serum of AlCl3-infected mice. Similarly, Xu *et al.* (2017) found that exposure to $AlCl_3$ resulted in elevated blood AST and ALT activity and induced liver histological damage. Prior research has indicated that in cases of liver injury, there is an elevation in the levels of AST and ALT, which are then discharged into the bloodstream. The high levels of AST and ALT indicate liver damage (Pratt and Kaplan, 2000).

The observed rise in blood ALT and AST levels suggests that exposure to $AlCl_3$ results in heightened permeability, injury, and necrosis of liver cells. Similarly, Türkez *et al.* (2010) found that ingesting $AlCl_3$ (34 mg/kg

body weight) increased blood AST and ALT levels. Al stress has been linked to alterations in blood lipid profiles. Following immobilization in rabbits, a marked increase in the blood's TC, LDL-c, VLDL-c, and TAG levels (Hamrayev *et al.*, 2021) were reported. Such changes were also reported in genetically modified mice (Haj-Mirzaian *et al.*, 2021). In rats, there has been a decrease in HDL-c concentration after immobilization, chronic unpredictable stressors, and restraint (da Silva Marques *et al.*, 2021). The application of chronic restraint in our study increased serum TC and TAG levels, did not change LDL-c or VLDL-c, and lowered HDL-c and FFA levels. Such results indicate the induction of dyslipidemia. This can be supported by Retem *et al.*, (2022), who stated that under stress, LDL-c levels rise while HDL-c levels fall. Rats under continuous restraint stress reported had much lower total cholesterol levels.

The effect of administration of ZnO-NPs on lipid profile is yet unclear. One study revealed that ZnO- NPs significantly improved TC and TAG levels (Abdulmalek *et al.*, 2021). These anti-hyperlipidemic activities of ZnO-NPs may be related to the nanoparticles' improving the affected pancreatic -cells' insulin-like nature. In our study, oral administration of ZnO-NPs increased HDL-c, LDL-c, VLDL-c, and FFA but not TC or TAG in handled rats. Oral administration of ZnO-NPs decreased TC and FFA but not TAG, LDL-c, or VLDL-c in chronic restraint-stressed rats while increasing HDL-c levels. The effect of ZnO-NPs on the lipid profile could be dose/route dependent. Administration of higher levels of ZnO-NPs (25 mg/kg and 50 mg/kg) increased serum levels of triglyceride (Naji *et al.*, 2023). Administration of comparably lesser levels of ZnO- NPs significantly decreased TAG levels (Karema El M *et al.*, 2020).

Any incompatibility between the antioxidant system and ROS generation and any increase in free radical species would result in oxidative damage to various cell components, including lipids, proteins, and nucleic acids. Al stress may disrupt the oxidant/antioxidant equilibrium, causing a high generation of free radicals while suppressing antioxidant capacity. The current findings, like previous studies, showed that oxidative lipid peroxidation marker (MDA) levels increased under prolonged restraint stress, whereas TAC levels decreased (Nguyen and Stamper, 2020).

The results of the antioxidant activity of ZnNPs analysis demonstrated a notable reduction in the levels of SOD and CAT, suggesting the presence of oxidative damage caused by $AlCl_3$. The treatment groups exhibited elevated levels of SOD and CAT, which aligns with the findings of a previous study that reported a substantial rise in SOD and CAT levels due to the administration of ZnNPs. Our investigation found that the scavenging activity of ZnONPs was superior to the other treatments, consistent with the findings of previous studies (Zhang *et al.*, 2022a), which reported that supplying the inclusion of the dietary ZnNPs enhances the activity of both SOD and CAT in the blood; however, Furthermore, research has indicated that ZnONPs at a 60 mg/kg dosage exhibit favorable Cu-Zn-SOD activity. Zinc oxide nanoparticles (ZnONPs) possess a notable antioxidant activity due to the presence of Zinc, a crucial component of superoxide dismutase (SOD). This enzyme effectively combats oxidative stress by rapidly eliminating superoxide free radicals. Zinc oxide nanoparticles (ZnONPs) exhibit antioxidant action by competing with iron and copper to bind to specific sites on cell membranes. This rivalry reduces the formation of free radicals, hence decreasing oxidative stress.

The oxidative impacts of ZnO-NPs depend on the dose of administration. Shehata *et al.* (2021) reported that ZnO-NPs significantly decreased the MDA level at a lower dose similar to the one used in our study. According to Li *et al.* (2024) ZnO-NPs can reduce MDA levels, increase antioxidant enzyme activity, and protect cell membrane integrity from oxidative stress damage. Furthermore, ZnO-NPs have a hepatoprotective impact at low dosages, either removing free radicals from the environment or stimulating antioxidant processes that detoxify free radicals (Hassan *et al.*, 2021). However, administering higher levels of ZnO-NPs was suggested to induce oxidative stress owing to a significant decrease in the activity of antioxidant enzymes and reduced blood TAC levels in rats. MDA and total oxidant status (TOS) levels have increased significantly after exposure to a high concentration of ZnO-NPs (Goma *et al.*, 2020).

Additionally, it is suggested that Zn enhances the synthesis of metallothionein, a protein crucial in neutralizing harmful free radicals (Giménez *et al.*, 2021). Zinc also activates antioxidant enzymes and proteins, including GPx and CAT (Koner *et al.*, 2021). The $AlCl_3$-challenged group exhibited a significant increase in proinflammatory cytokines, as indicated by this study.

Administration of ZnNPs reduced the levels of proinflammatory cytokines, specifically interleukin-2 (IL-2) and tumor necrosis factor-alpha (TNF-α). This study confirms previous findings (Zhang *et al.*, 2022a) that zinc oxide nanoparticles decrease levels of inflammatory molecules (IL-2 and TNF-α) in the blood. This anti-inflammatory effect of Zinc is likely due to activation of the Nrf2/HO-1 signaling pathway (Wang *et al.*, 2024).

Nrf2 activation reduces the production of proinflammatory cytokines and promotes the production of immunoglobulins. Furthermore, (Yen *et al.*, 2021; Zhang *et al.*, 2022b) have indicated that activating the Nrf2/HO-1 pathway effectively halts the inflammatory responses mediated by TLR4. Research suggests that the antioxidant effect of ZnNPs improves growth performance.

Conclusions: Aluminum is crucial in inducing oxidative and inflammatory stress, disrupting the neurological system's homeostasis. The findings of this study suggest that the administration of ZnNPs as antioxidant agents in mice treated with $AlCl_3$ had beneficial effects. These agents were able to reduce the ROS response and enhance the enzymatic and nonenzymatic systems (SOD and GSH). The evidence indicates that ZnNPs can mitigate the toxicity of $AlCl_3$ in albino mice and improve the neurological and antioxidant properties.

Competing interests: The authors declare that they have no competing interests.

Acknowledgements: The authors gratefully acknowledge Princess Nourah bint Abdulrahman University Researchers Supporting Project number (PNURSP2024R367), Princess

Nourah bint Abdulrahman University, Riyadh, Saudi Arabia. The authors extend their appreciation to the Deanship of Research and Graduate Studies at King Khalid University for funding this work through Large Research Project under Grant number: RGP2/570/45.

Authors contributions: Conceptualization, NAB, HKAG, SMA, and MA, formal analysis, NAB, WAK, and KMW, investigation, NAB, AO, NB, MA, and NA, data curation, NAB, HKAG, SMA, MA, AO, NB, MA, NA, NFA, SSA, AMA, and AA, writing original draft preparation, NAB, AO, NB, MA, NA, NFA, SSA, AMA, and AA, writing final manuscript and editing, NAB, HKAG, SMA, MA, AO, NB, MA, NA, NFA, and SSA, visualization and methodology, NAB, HKAG, SMA, MA, AO, NB, MA, NA, NFA, SSA, AMA, AA, WAK, and KMW. All authors have read and agreed to the published version of the manuscript.

REFERENCES

Abdel-Moneim A-ME, El-Saadony MT, Shehata AM, *et al.,* 2022. Antioxidant and antimicrobial activities of *Spirulina platensis* extracts and biogenic selenium nanoparticles against selected pathogenic bacteria and fungi. Saudi J Biol Sci 29:1197-1209.

Abdulmalek S, Eldala A, Awad D, *et al.,* 2021. Ameliorative effect of curcumin and zinc oxide nanoparticles on multiple mechanisms in obese rats with induced type 2 diabetes. Sci Rep 11:20677.

AbouAitah K, Allayh AK, Wojnarowicz J, *et al.,* 2021. Nanoformulation composed of ellagic acid and functionalized zinc oxide nanoparticles inactivates DNA and RNA viruses. Pharmaceutics 13:2174.

Al-Amin MM, Reza HM, Saadi HM, *et al.,* 2016. Astaxanthin ameliorates aluminum chloride-induced spatial memory impairment and neuronal oxidative stress in mice. Eur J Pharmacol 777:60-69.

Alowaiesh BF, Alhaithloul HAS, Saad AM, *et al.,* 2023. Green biogenic of silver nanoparticles using polyphenolic extract of olive leaf wastes with focus on their anticancer and antimicrobial activities. Plants 12:1410.

Arisha AH, Ahmed MM, Kamel MA, *et al.,* 2019. Morin ameliorates the testicular apoptosis, oxidative stress, and impact on blood–testis barrier induced by photo-extracellularly synthesized silver nanoparticles. Environ Sci Pollut Res 26:28749-28762.

Bahrampour K, Ziaei N, Esmaeilipour O, 2021. Feeding nano particles of vitamin C and zinc oxide: Effect on growth performance, immune response, intestinal morphology and blood constituents in heat stressed broiler chickens. Livest Sci 253:104719.

Bakhtiari M, Panahi Y, Ameli J, *et al.,* 2017. Protective effects of flavonoids against Alzheimer's disease-related neural dysfunctions. Biomed Pharmacother 93:218-229.

Bakoyiannis I, Daskalopoulou A, Pergialiotis V, *et al.,* 2019. Phytochemicals and cognitive health: Are flavonoids doing the trick? Biomed Pharmacother 109:1488-1497.

Bami MK, Afsharmanesh M, Espahbodi M, *et al.,* 2022. Effects of dietary nano-selenium supplementation on broiler chicken performance, meat selenium content, intestinal microflora, intestinal morphology, and immune response. J Trace Elem Med Biol 69:126897.

Blinova I, Muna M, Heinlaan M, *et al.,* 2020. Potential hazard of lanthanides and lanthanide-based nanoparticles to aquatic ecosystems: Data gaps, challenges and future research needs derived from bibliometric analysis. Nanomaterials 10:328.

Bosnjak MC, Dobovski-Poslon M, Bibic Z, *et al.,* 2019. The influence of chronic stress on health and coping mechanisms. Sanamed 14:97-101.

Burtis CA, Ashwood E, 1999. Tietz Textbook of Clinical Chemistry. 3rd Edition, W. B. Saunders Co., Philadelphia 29-150.

Cirovic A, Cirovic A, 2022. Aluminum bone toxicity in infants may be promoted by iron deficiency. J Trace Elem Med Biol 71:126941.

da Silva Marques JG, Antunes FTT, da Silva Brum LF, *et al.,* 2021. Adaptogenic effects of curcumin on depression induced by moderate and unpredictable chronic stress in mice. Behav Brain Res 399:113002.

Doroszkiewicz J, Farhan JA, Mroczko J, *et al.,* 2023. Common and trace metals in Alzheimer's and Parkinson's diseases. Int J Mol Sci 24(21): 15721.

El-Hawwary SS, Abd Almaksoud HM, Saber FR, *et al.,* 2021. Green-synthesized zinc oxide nanoparticles, anti-Alzheimer potential and the metabolic profiling of Sabal blackburniana grown in Egypt supported by molecular modelling. RSC Adv 11:18009-18025.

El-Katcha MI, Soltan MA, Arafa MM, *et al.,* 2018. Impact of dietary replacement of inorganic Zinc by organic or nano sources on productive performance, immune response and some blood biochemical constituents of laying hens. Alexandria J Vet Sci 59(1): 48-59.

El-Saadony MT, Alkhatib FM, Alzahrani SO, *et al.,* 2021a. Impact of mycogenic zinc nanoparticles on performance, behavior, immune response, and microbial load in *Oreochromis niloticus*. Saudi J Biol Sci 28:4592-4604.

El-Saadony MT, El-Wafai NA, El-Fattah HIA, *et al.,* 2019. Biosynthesis, optimization and characterization of silver nanoparticles using a soil isolate of *Bacillus pseudomycoides* MT32 and their antifungal activity against some pathogenic fungi. Adv Anim Vet Sci 7:238-249.

El-Saadony MT, Saad AM, Elakkad HA, *et al.,* 2022. Flavoring and extending the shelf life of cucumber juice with aroma compounds-rich herbal extracts at 4°C through controlling chemical and microbial fluctuations. Saudi J Biol Sci 29:346-354.

El-Saadony MT, Saad AM, Najjar AA, et al., 2021b. The use of biological selenium nanoparticles to suppress *Triticum aestivum* L. crown and root rot diseases induced by *Fusarium* species and improve yield under drought and heat stress. Saudi J Biol Sci 28:4461-4471.

El-Saadony MT, Saad AM, El-Wafai NA, *et al.,* 2023. Hazardous wastes and management strategies of landfill leachates: A comprehensive review. Enviro Technol Innov 31:103150.

Ermakov V, Jovanović L, 2022. Biological role of trace elements and viral pathologies. Geochem Int 60:137-153.

Fatima A, Zaheer T, Pal K, *et al.,* 2024. Zinc oxide nanoparticles significant role in poultry and novel toxicological mechanisms. Biolog Trace Elem Res 202(1): 268-290.

Gauba A, Hari SK, Ramamoorthy V, *et al.,* 2023. The versatility of green synthesized zinc oxide nanoparticles in sustainable agriculture: A review on metal-microbe interaction that rewards agriculture. Physiol Mol Plant Pathol 125:102023.

Ghaffari H, Tavakoli A, Moradi A, *et al.,* 2019. Inhibition of H1N1 influenza virus infection by zinc oxide nanoparticles: another emerging application of nanomedicine. J Biomed Sci 26:1-10.

Giménez VMM, Bergam I, Reiter RJ, *et al.,* 2021. Metal ion homeostasis with emphasis on Zinc and copper: Potential crucial link to explain the non-classical antioxidative properties of vitamin D and melatonin. Life Sci 281:119770.

Gökmen S,Gül B, 2023. Aluminum and toxicity. Vet J KU 2:52-64.

Goma AA, Tohamy HG, El-Kazaz SE, *et al.,* 2020. Insight study on the comparison between Zinc Oxide nanoparticles and its bulk impact on reproductive performance, antioxidant levels, gene expression, and histopathology of testes in male rats. Antioxidants 10:41.

Gomaa AA, Makboul RM, El-Mokhtar MA, *et al.,* 2019. Terpenoid-rich Elettaria cardamomum extract prevents Alzheimer-like alterations induced in diabetic rats via inhibition of GSK3β activity, oxidative stress and proinflammatory cytokines. Cytokine 113:405-416.

Gupta J, Irfan M, Ramgir N, *et al.,* 2022. Antiviral activity of zinc oxide nanoparticles and tetrapods against the Hepatitis E and Hepatitis C viruses. Front Microbiol 13:881595.

Haj-Mirzaian A, Ramezanzadeh K, Shariatzadeh S, *et al.,* 2021. Role of hypothalamic-pituitary adrenal-axis, toll-like receptors, and macrophage polarization in pre-atherosclerotic changes induced by social isolation stress in mice. Sci Rep 11:19091.

Hamrayev H, Shameli K, Korpayev S, 2021. Green synthesis of zinc oxide nanoparticles and its biomedical applications: A review. J Res Nanosci Nanotechnol 1:62-74.

Hao W, Hao C, Wu C, *et al.,* 2022. Aluminum induced intestinal dysfunction via mechanical, immune, chemical and biological barriers. Chemosphere 288:132556.

Hassan AA, El-Ahl RMS, Oraby NH, *et al.,* 2021. Zinc nanomaterials: Toxicological effects and veterinary applications. In: Zinc-based nanostructures for environmental and agricultural applications: Elsevier. p 509-541.

Hassan HS, Abol-Fotouh D, Salama E, *et al.,* 2022. Assessment of antimicrobial, cytotoxicity, and antiviral impact of a green zinc oxide/activated carbon nanocomposite. Sci Rep 12:8774.

Homaeigohar S, Liu X, Elbahri M, 2023. Antiviral polysaccharide and antiviral peptide delivering nanomaterials for prevention and treatment of SARS-CoV-2 caused COVID-19 and other viral diseases. J Control Release 358:476-497.

House JA, Wilson TM, Nakashly SE, *et al.,* 1990. The isolation of lumpy skin disease virus and bovine herpesvirus-from cattle in Egypt. J Vet Diagn Invest 2:111-115.

Jiang J, Pi J, Cai J, 2018. The advancing of zinc oxide nanoparticles for biomedical applications. Bioinorg Chem Appl 2018:1062562.

Karema El M S, Attia AM, El-Banna SG, *et al.,* 2020. Anti-dyslipidemic effect of zinc oxide nanoparticles against cyclophosphamide induced dyslipidemia in male albino rats. GMS Ger Med Sci 1(1):55-63.

Khamis T, Abdelkhalek A, Abdellatif H, *et al.,* 2023. BM-MSCs alleviate diabetic nephropathy in male rats by regulating ER stress, oxidative stress, inflammation, and apoptotic pathways. Front Pharmacol 14:1265230.

Koner D, Banerjee B, Kumari A, *et al.,* 2021. Molecular characterization of superoxide dismutase and catalase genes, and the induction of antioxidant genes under the zinc oxide nanoparticle-induced oxidative stress in air-breathing magur catfish (Clarias magur). Fish Physiol Biochem 47:1909-1932.

Krupińska I. 2020, Aluminium drinking water treatment residuals and their toxic impact on human health. Molecules 25:641.

Kumar S, Ansari S, Narayanan S, et al., 2023. Antiviral activity of zinc against hepatitis viruses: current status and future prospects. Front Microbiol 14: 1218654.

Laabbar W, Abbaoui A, Elgot A, *et al.,* 2021. Aluminum induced oxidative stress, astrogliosis and cell death in rat astrocytes, is prevented by curcumin. J Chem Neuroanat 112:101915.

Laabbar W, Elgot A, Kissani N, *et al.,* 2014. Chronic aluminum intoxication in rat induced both serotonin changes in the dorsal raphe nucleus and alteration of glycoprotein secretion in the subcommissural organ: Immunohistochemical study. Neurosci Lett 577:72-76.

Li Y, Pan M, Meng S, *et al.,* 2024. The effects of zinc oxide nanoparticles on antioxidation, inflammation, tight junction integrity, and apoptosis in heat-stressed bovine intestinal epithelial cells in vitro. Biol Trace Elem Res 202:2042-2051.

Mathur S, Singh D,Ranjan R, 2022. Remediation of heavy metal (loid) contaminated soil through green nanotechnology. Front Sustain Food Syst 6:932424.

Matuszczak M, Kiljańczyk A, Marciniak W, *et al.,* 2024. Zinc and Its antioxidant properties: The potential use of blood zinc levels as a marker of cancer risk in brca1 mutation carriers. Antioxidants 13:609.

Mekky AE, Farrag AA, Hmed AA, *et al.,* 2021. Preparation of zinc oxide nanoparticles using Aspergillus niger as antimicrobial and anticancer agents. J Pure Appl Microbiol 15:1547-1566.

Melk MM, El-Hawary SS, Melek FR, *et al.,* 2021. Antiviral activity of zinc oxide nanoparticles mediated by Plumbago indica L. extract against herpes simplex virus type 1 (HSV-1). Int J Nanomed 16: 8221–8233.

Mishra PK, Mishra H, Ekielski A, *et al.,* 2017. Zinc oxide nanoparticles: a promising nanomaterial for biomedical applications. Drug Discov Today 22:1825-1834.

Mohd Yusof H, Abdul Rahman NA, Mohamad R, *et al.,* 2021. Antibacterial potential of biosynthesized zinc oxide nanoparticles against poultry-associated foodborne pathogens: an in vitro study. Animals 11:2093.

Montoya-Castrillón M, Serna-Vasco KJ, Pinilla L, *et al.,* 2021. Isolation and Characterization of filamentous fungi from wood and soil samples of "La Lorena", Sonsón, Antioquia (Colombia), natural reserve. Dyna 88:171-180.

Moss DW, 1982. Alkaline phosphatase isoenzymes. Clin Chem 28:2007-2016.

Moustafa A,Arisha AH, 2020. Swim therapy-induced tissue specific metabolic responses in male rats. Life Sci 262:118516.

Naji RM, Bashandy MA, Fathy AH, 2023. Ameliorative effects of some natural antioxidants against blood and cardiovascular toxicity of oral subchronic exposure to silicon dioxide, aluminum oxide, or zinc oxide nanoparticles in wistar rats. Int J Food Sci 2023:8373406.

Nguyen NU, Stamper BD, 2020. A template-based approach for guiding and refining the development of cinnamon-based phenylpropanoids as drugs. Molecules 25:4629.

NRC, 1994. Nutrient requirements of poultry: 1994: National Academies Press.

Ogbuewu IP, Mbajiorgu CA, 2023. Potentials of dietary zinc supplementation in improving growth performance, health status, and meat quality of broiler chickens. Biol Trace Elem Res 201:1418-1431.

Olivares-Bañuelos T, Gutiérrez-Rodríguez AG, Méndez-Bellido R, *et al.,* 2019. Brown seaweed Egregia menziesii's cytotoxic activity against brain cancer cell lines. Molecules 24(2): 260.

OIE, 2010. (World Organization for Animal Health). "Lumpy skin disease," OIE Terr. Anim. Heal. Code, May, pp. 1–4.

Prasad RD, Charmode N, Shrivastav OP, *et al.,* 2021. A review on concept of nanotechnology in veterinary medicine. ES Food Agrofor 4:28-60.

Pratt DS,Kaplan MM, 2000. Evaluation of abnormal liver-enzyme results in asymptomatic patients. New England J Med 342:1266-1271.

Praveen A, Singh S, Sharma VK, 2023. Action of nanoparticles in the amelioration of heavy metal phytotoxicity. Cereal Res Commun 51:537-544.

Rao X, Huang X, Zhou Z, *et al.,* 2013. An improvement of the 2ˆ (–delta delta CT) method for quantitative real-time polymerase chain reaction data analysis. Biostat Bioinforma Biomath 3(3): 71–85.

Renke G, Almeida VBP, Souza EA, *et al.,* 2023. Clinical outcomes of the deleterious effects of aluminum on neuro-cognition, inflammation, and health: a review. Nutrients 15:2221.

Retem C, Djemli S, Chebbah F, *et al.,* 2022. Assessment of Coercive Stress on the Behavioral, Exploratory and Metabolic Response in the Wistar Rats. Phcog Commn 12:52-55.

Saad AM, Sitohy MZ, Ahmed AI, *et al.,* 2021. Biochemical and functional characterization of kidney bean protein alcalase-hydrolysates and their preservative action on stored chicken meat. Molecules 26:4690.

Saad AM, Sitohy MZ, Sultan-Alolama MI, *et al.,* 2022. Green nanotechnology for controlling bacterial load and heavy metal accumulation in Nile tilapia fish using biological selenium nanoparticles biosynthesized by *Bacillus subtilis* AS12. Front Microbiol 13:1015613.

Schneiderhan W, Diaz F, Fundel M, *et al.,* 2007. Pancreatic stellate cells are an important source of MMP-2 in human pancreatic cancer and accelerate tumor progression in a murine xenograft model and CAM assay. J Cell Sci 120:512-519.

Seyfi R, Kahaki FA, Ebrahimi T, *et al.,* 2020. Antimicrobial peptides (AMPs): roles, functions and mechanism of action. Int J Pept Res Ther 26:1451-1463.

Shaba EY, Jacob JO, Tijani JO, *et al.,* 2021. A critical review of synthesis parameters affecting the properties of zinc oxide nanoparticle and its application in wastewater treatment. Appl Water Sci 11(48): 1-41.

Shamim A, Mahmood T, Abid MB, 2019. Biogenic synthesis of zinc oxide (ZnO) nanoparticles using a fungus (Aspergillus niger) and their characterization. Int J Chem11:119.

Sharifan H, Moore J, Ma X, 2020. Zinc oxide (ZnO) nanoparticles elevated iron and copper contents and mitigated the bioavailability of lead and cadmium in different leafy greens. Ecotoxicol Environ Saf 191:110177.

Skalny AV, Aschner M, Lei XG, *et al.,* 2021. Gut microbiota as a mediator of essential and toxic effects of zinc in the intestines and other tissues. Int J Mol Sci 22(23): 13074.

Suvarna M, Niranjan U, 2013. Classification methods of skin burn images. Int J Comp Sci Info Tech 5(1):109.

Türkez H, Yousef MI,Geyikoglu F, 2010. Propolis prevents aluminium-induced genetic and hepatic damages in rat liver. Food ChemToxicol 48:2741-2746.

Ungureanu EL,Mustatea G, 2022. Toxicity of heavy metals. In: Environmental impact and remediation of heavy metals: IntechOpen.

Wang P, Gao L, Ma T, *et al.,* 2024. MicroRNA-1225-5p Promotes the Development of Fibrotic Cataracts via Keap1/Nrf2 Signaling. Curr Eye Res 49:591-604.

Willhite CC, Karyakina NA, Yokel RA, *et al.,* 2014. Systematic review of potential health risks posed by pharmaceutical, occupational and consumer exposures to metallic and nanoscale aluminum, aluminum oxides, aluminum hydroxide and its soluble salts. Crit Rev Toxicol 44:1-80.

Xu F, Liu Y, Zhao H, *et al.,* 2017. Aluminum chloride caused liver dysfunction and mitochondrial energy metabolism disorder in rat. J Inorg Biochem 174:55-62.

Yen I-C, Tu Q-W, Chang T-C, *et al.,* 2021. 4-Acetylantroquinonol B ameliorates nonalcoholic steatohepatitis by suppression of ER stress and NLRP3 inflammasome activation. Biomed Pharmacother 138:111504.

Zeedan G, El-Razik K, Allam A, *et al.,* 2020. Evaluations of potential antiviral effects of green zinc oxide and silver nanoparticles against bovine herpesvirus-1. Adv Anim Vet Sci 8:433-443.

Zeedan GSG, Mahmoud AH, Abdalhamed AM, *et al.,* 2019. Detection of lumpy skin disease virus in cattle using real-time polymerase chain reaction and serological diagnostic assays in different governorates in Egypt in 2017. Vet World 12:1093.

Zhang J, Li Z, Yu C, *et al.,* 2022a. Efficacy of using zinc oxide nanoparticle as a substitute to antibiotic growth promoter and zinc sulphate for growth performance, antioxidant capacity, immunity and intestinal barrier function in broilers. Ital J Anim Sci 21:562-576.

Zhang J, Yu C, Li Z, *et al.,* 2022b. Effects of zinc oxide nanoparticles on growth, intestinal barrier, oxidative status and mineral deposition in 21-day-old broiler chicks. Biol Trace Elem Res 200:1826-1834.

Zhou J, Hu Z, Zabihi F, et al., 2020a. Progress and perspective of antiviral protective material. Adv Fiber Mater 2:123-139.

Zhou L, Abouelezz K, Momenah MA, *et al.,* 2024. Dietary *Paenibacillus polymyxa* AM20 as a new probiotic: Improving effects on IR broiler growth performance, hepatosomatic index, thyroid hormones, lipid profile, immune response, antioxidant parameters, and caecal microorganisms. Poult Sci 103:103239.

Zhou P, Adeel M, Shakoor N, et al., 2020b. Application of nanoparticles alleviates heavy metals stress and promotes plant growth: An overview. Nanomaterials 11:26.